European Journal of Pharmaceutical Sciences 187 (2023) 106491

Contents lists available at ScienceDirect

European Journal of Pharmaceutical Sciences

journal homepage: www.elsevier.com/locate/ejps

Formulation and characterization of pramipexole containing buccal films for using in Parkinson's disease

Krisztián Pamlényi [a], Géza Regdon Jr. [a,*], Orsolya Jójárt-Laczkovich [a], Dániel Nemes [b], Ildikó Bácskay [b], Katalin Kristó [a]

[a] Institute of Pharmaceutical Technology and Regulatory Affairs, University of Szeged, Eötvös u. 6., H-6720 Szeged, Hungary
[b] Department of Pharmaceutical Technology, University of Debrecen, Nagyerdei krt. 98., H-4032 Debrecen, Hungary

ARTICLE INFO

Keywords:
Mucoadhesive buccal films
Drug delivery system
Alginate
Pramipexole
Parkinson's disease
Swallowing problems

ABSTRACT

Parkinson's disease (PD) is neurodegenerative chronic illness which affects primarily the elderly over 45 years of age. The symptoms can be various, both non-motor and motor symptoms can appear. The biggest problem in the treatment of the disease is the difficulty in swallowing for the patients. However, buccal patches can solve this problem because the patients do not have to swallow the dosage form, and during application, the API can absorb from the area of the buccal mucosa quickly without causing a foreign body sensation. In our present study, we focused on the development of buccal polymer films with pramipexole dihydrochloride (PR). Films with different compositions were formulated and their mechanical properties and chemical interactions were investigated. The biocompatibility of the film compositions was examined on the TR146 buccal cell line. The permeation of PR was also monitored across the TR146 human cell line. It can be stated that the plasticizer can enhance the thickness and the breaking hardness of the films, while not decreasing their mucoadhesivity significantly. All formulations proved to have cell viability higher than 87%. Finally, we found the best composition (3% SA+1% GLY-PR-Sample1) which can be applied on the buccal mucosa in the treatment of PD.

1. Introduction

Parkinson's disease (PD) is one of the most common neurodegenerative disorders (Lee and Gilbert, 2016). It is caused by the loss of dopaminergic neurons in the substantia nigra and pars compacta, which can result in dopamine deficiency, and on the other hand by the accumulation of misfolded α-synuclein, which can create intracellular inclusions (Lewis bodies) in these different areas of the brain (Balestrino and Schapira, 2020; Poewe et al., 2017). The clinical picture of PD varies widely, including both motor and non-motor symptoms. Motor symptoms are characterized by tremor, muscle rigidity, bradykinesia, akinesia, postural instability, eye movements, micrographia, etc. (Aarsland et al., 2017; Balestrino and Schapira, 2020). Non-motor symptoms appear in the form of dementia, depression, anxiety, hallucinations, sexual dysfunction, constipation, delayed stomach emptying, dysphagia, disturbances of sleep and wakefulness (Park and Stacy, 2009; Pfeiffer, 2016; Sprenger and Poewe, 2013).

The current treatment of PD focuses on replacing the dopamine level from an external source (Levodopa-L-DOPA) or applying a dopamine agonist API which can stimulate the dopamine receptors in the central nervous system (Antonini et al., 2009; de Souza Silva et al., 1997; Goberman and Blomgren, 2003; Mercuri and Bernardi, 2005; Stowe et al., 2008; Zanettini et al., 2007). In addition, there are other therapeutic targets in the treatment of PD (Barrett et al., 2021; Hubsher et al., 2012; Katzenschlager et al., 2002).

Pramipexole dihydrochloride (PR) is a non-ergot dopamine agonist compound (Shin et al., 2009). It can bind to the different types of dopamine receptors (D2, D3, D4) (Lemke et al., 2006; Whitton et al., 2020). Pramipexole is most often applied in PD, but it is also used in restless legs syndrome (Allen et al., 2014). PR is taken orally alone or in combination with levodopa. The bioavailability of PR is high, more than 90% by the oral administration route (Diao et al., 2010). However, a large number of patients suffer from swallowing problems (dysphagia) as a result of PD. Many patients are not able to swallow tablets or capsules, therefore the therapy cannot be successful. In these cases, buccal polymer tablets or films can be used as an alternative option to deliver the API to the systemic circulation without swallowing.

The buccal administration route has further positive properties (Alves et al., 2020). A smaller dose of the active compound can be used

* Corresponding author.
E-mail address: geza.regdon@pharm.u-szeged.hu (G. Regdon).

https://doi.org/10.1016/j.ejps.2023.106491
Received 7 December 2022; Received in revised form 15 May 2023; Accepted 5 June 2023
Available online 9 June 2023

Abbreviations

PD	Parkinson's disease
PR	pramipexole dihydrochloride
SA	sodium alginate
GLY	Glycerol
HPMC	hydroxypropyl methylcellulose
API	active pharmaceutical ingredient
FT-IR	Fourier-Transform Infrared Spectroscopy
SD	standard deviation
HBSS	Hank's balanced salt solution
AC	apical compartment
BC	basolateral compartment
P_{app}	apparent permeability
FSC-SSC	forward and side scatter
SEM	standard error of the mean

in the buccal drug delivery system because the API is not metabolized in the liver, it is able to enter the systemic circulation immediately (Fonseca-Santos and Chorilli, 2018; Hanif et al., 2015). Buccal products can be applied easily and painlessly (Nair et al., 2018). The advantage of the polymer film over the tablet is that the film cannot cause foreign body sensation in the mouth, and patients do not notice the application of the product (El-Maghraby and Abdelzaher, 2015). In pediatrics and geriatrics, this property can be exploited for successful drug delivery (Boateng, 2017; Chachlioutaki et al., 2020; Montero-Padilla et al., 2017). However, it is also true that buccal films have a limitation because they only allow the incorporation of a small amount of API. Moreover, the surface of the buccal mucosa is a small area, therefore buccal films should be small to attach to it. On the other hand, the transport across buccal cells also has limitations. In the case of a high amount of API, the API cannot be fully absorbed. In addition, during application, the buccal film is in contact with the saliva in the buccal cavity. We have to avoid the API dissolving from the film in the direction of the buccal cavity because then we would swallow the API. A solution to the problem can be a cover layer which is located on the side of the film towards the oral cavity and prevents the API from being dissolved by the saliva.

In our previous works, we formulated buccal films with cetirizine dihydrochloride (Pamlényi et al., 2022), and we found promising compositions during our research. Films with 3% polymer concentration, 3% SA + 1% GLY-CTZ and 3% SA + 1% GLY-CTZ proved to be suitable for use as a drug delivery system. Therefore, in this project, we intend to apply PR as an active agent in the polymer film system, which can also be used on the buccal mucosa to improve the success of the current Parkinson's therapy with the PR compound. The novelty of this work is that we developed a buccal film from PR in PD. Due to swallowing difficulties, the current drug therapy for PD can be significantly improved with the buccal film, therefore that was our main goal. A further novelty of our work is that we investigated many properties of the prepared films extensively. During this project, we examined the physical properties of the films which can influence the application, such as the finger placement of the films or their adhesivity to mucin. We also aimed to investigate the chemical properties of the films to determine the interactions between the components of the patches, which can explain some phenomena, for example, hydrogen bonds and cross-linking can be created between the components of films, the excipients, especially the API can undergo decomposition and new materials can be formed due to the interactions, and these phenomena can influence the stability of the product. Furthermore, we studied the permeability of PR from the film on the TR 146 buccal cell line to determine the quantity of the transported API which can have an effect *de facto*. It is also important to examine the cytotoxicity of the films because it can influence the outcome of further development. Our final aim is to find the best composition, which has good mechanical properties, high permeability and appropriate cytotoxicity.

Fig. 1. Camera photo about Sample 4. (For interpretation of the references to color in this figure legend, the reader is referred to the web version of this article.)

2. Materials and methods

2.1. Materials

SA (Biochemica GmbH, Darmstadt, Germany) (10,000 – 600,000 g/mol) and HPMC (Metolose® 2208, Shin Etsu Chemical Co., Ltd., Tokyo, Japan) (>500,000 g/mol) were used as a film forming agent in the polymer film. GLY 85% (w/w%) was added to the film as a plasticizer (pH. Eur.8.). PR (pH. Eur. 8.) was the API, which was a gift from KRKA, d.d., (Novo Mesto, Slovenia). Mucin (Carl Roth GmbH + Co. KG, Karlsruhe, Germany) (10 w/w%) dispersion was used in the *in vitro* mucoadhesion test.

Table 1
Composition of different PR containing films (The table reports the composition of the prepared polymer solution).

Samples	SA (w/w%)	HPMC (w/w%)	GLY (w/w%)	PR (w/w%))
1	1	2	1	0.0793
2	1	2	2	0.0793
3	1	2	3	0.0793
4	1.5	1.5	1	0.0793
5	1.5	1.5	2	0.0793
6	1.5	1.5	3	0.0793
7	2	1	1	0.0793
8	2	1	2	0.0793
9	2	1	3	0.0793

2.2. Preparation of buccal films

The films were prepared at room temperature with the solvent casting method. As the first step of preparation, SA (1, 1.5, 2 w/w%) was dissolved in distilled water and mixed (900 rpm) at room temperature with an overhead stirrer (Velp Scientifica Srl, Usmate, Italy). The mixing speed of the solution was decreased (500 rpm) and PR was incorporated in the polymer solution (0.0793 w/w%) for 5 h. As the third step, HPMC (1, 1.5. 2 w/w%) was added to the solution with mixing. In the fourth step, GLY was added to the solution. Mixing was stopped and it was placed in an ultrasonic unit (Elmasonic S 30 (H), Wetzikon, Switzerland) for 30 min to help the number and the size of air bubbles reduce and remove from the solution. The solution (pH = 6.7–7.0, viscosity: 140–173 mPa•s) was cast onto a glass surface in Petri dishes (7.6 cm diameter), with 10 g of solution/dish, then it was dried at room temperature (24.4 ± 0.5 °C). The dried polymer films were removed from the surface and placed in closed containers (24.4 ± 1 °C, 60 ± 2% RH). In Fig. 1. the camera photos of Sample 4 (1.5% SA + 1.5% HPMC + 1% GLY-CTZ) can be seen.

Table 1 shows the different compositions of the prepared polymer films. All film compositions contain PR. The weight of PR was 0.7 mg/cm^2

2.3. Thickness of the films

The thickness of the polymer films was measured with a screw micrometer (Mitutoyo Co. Ltd, Tokyo, Japan), sensitivity was 0.001 mm. Eight points were selected randomly from all films (n = 8). The means and standard deviations (SD) were evaluated from these data (Pamlényi et al., 2021).

2.4. Moisture content of the films

The moisture content of the buccal films was measured. The residual water amount of the films was investigated with a moisture analyser (RADWAG MAC 50/NH, Poland). Pieces of films of 5 cm^2 were examined. The maximum temperature was 105 °C. The duration of the test was 8 min. The test was performed three times (n = 3) for each combination of films. The means and standard deviations (SD) were evaluated from these data.

2.5. Tensile strength (hardness) of films

Tensile strength was measured with a texture analyser developed in our department (Kelemen et al., 2015). The equipment has different sample holders and two different probes (needle-like probe, rod-like probe). The equipment has a fix disk and a moving sample holder. Depending on the investigation, a different sample holder can be used and during the measurement the force, moving speed and time can be registered. The needle-like probe was used in the hardness test. The probe was moved downward at constant speed, and the sample was fixed on the bottom part of equipment. The probe went through the film and the equipment detected the time and force during the investigation. The test was finished when the film was broken. The films were cut to 4 mm^2. The test was performed eight times (n = 8) for each combination of films. The means and standard deviations were calculated. The equipment was presented in our earlier works (Ibrahim et al., 2020; Kelemen et al., 2015).

2.6. In vitro mucoadhesivity of films

Mucoadhesion was measured with the same texture analyser with different settings and assembling modifications. In this measurement, the rod-like sample holder with a diameter of 5 mm was applied. A double-faced adhesive tape was fixed on the surface of the sample holder, and the polymer film was fixed on the other face of the adhesive tape with a film size of 78.5 mm^2. A disk with a 35-mm diameter was fixed on the bottom part of the tester and 40 µl of freshly prepared mucin dispersion (10 w/w%) was spread on it. The rod-like sample holder was moved downward and pressed the polymer film to the mucin-covered bottom disk with 30 ± 0.1 N for 30 s. This steady state part can be detected in the force-time curve. After that, the sample holder was moved upwards, the force was decreased until the sample started to separate from mucin, which can be seen as a well-defined peak in the force-time curve, which means the in vitro mucoadhesivity force of the films. The test was repeated eight times (n = 8) and the means and standard deviations were calculated (Kelemen et al., 2020).

2.7. Contact angle measurement and surface free energy (SFE)

4 cm^2 polymer films were placed on the microscope glass slides. One drop of distilled water and diiodomethane were used to measure the contact angle (Θ) of polymer films for 15 s, with the circle fitting method, by using a contact angle apparatus (OCA20-DataPhysics Instrument GmbH, Filderstadt, Germany). One drop of different liquids was applied, the volume of which was 10 µl and 5 µl in the case of distilled water and diiodomethane, respectively (Pamlényi et al., 2021).

The means and standard deviations (SD) were calculated from five identical samples of each combination of films (n = 5). The means and standard deviations were used to calculate the surface free energy of films. Surface free energy was calculated with Wu's method. This method defines the amounts of the polar (γ^p) and the dispersive (γ^d) components of solids. The SFE of solids can be calculated by using the following connection if the two parameters and the contact angle of the solid are known:

$$(1+\cos\Theta)\cdot\gamma = \frac{4\left(\gamma_s^d\cdot\gamma_l^d\right)}{\gamma_s^d+\gamma_l^d} + \frac{\left(\gamma_s^p\cdot\gamma_l^p\right)}{\gamma_s^p+\gamma_l^p}$$

where Θ is the contact angle of the solid-liquid surface, γ_l is the liquid surface tension, γ_s is the solid surface energy, which is the sum of their polar and dispersive components. According to Wu, the SFE of distilled water is 72.8 m N/m (polar part (γ^p) = 50.2 mN/m; dispersive part (γ^d) = 22.6 mN/m), while the SFE of diiodomethane is 50.8 mN/m (polar part (γ^p) = 1.8 mN/m; dispersive part (γ^d) = 49.0 mN/m) (Gottnek et al., 2013).

Knowing the polar and the dispersive parts of polymer films, the polarity of films can be established by using the following formula:

Polarity (%) = (γ^p (mN/m)/γ^{tot} (mN/m)) x 100 where γ^{tot} (mN/m) = γ^p (mN/m) + γ^d (mN/m)

2.8. Dissolution test

Two pieces of polymer films of a size of 1 cm^2 (containing in total 1.4 mg of PR) were measured in the dissolution test. In the case of one piece of film (0.7 mg - therapeutic dose), the detection of the amount of PR is not possible due to the low absorbance value. The dissolution test was

performed by a VELP (Scientifica Multi-HS 6/15 Digital, Usmate Velate, Italy) Multi-position Hot Plate Magnetic Stirrer in a 100 ml glass lab beaker at a mixing speed of 100 rpm. 50 ml of 0.05 M phosphate buffer (pH = 6.8) was used as dissolution medium, its temperature was 37 °C. The composition of the phosphate buffer was 1.00 g/L of KH_2PO_4, 2.00 g/L of K_2HPO_4, 8.50 g/L NaCl. Aliquots of 5 ml were analyzed in 5, 10, 15, 20, 30, 40, 50, 60, 90, 120 min with Genesys 10S UV–VIS (Thermo Fisher Scientific, Waltham, MA, USA) UV-spectrophotometry at $\lambda = 262$ nm wavelength (calibration equation: $y = 0.0297 \bullet x$, x = concentration: μg/ml, y = absorbance; $R^2 = 0.9981$). The removed volume was replaced with pH = 6.8 phosphate buffer.

2.9. FT-IR spectroscopy

The Fourier-Transform Infrared Spectra of the excipients and the polymer films were analyzed with an Avatar 330 FT-IR apparatus (Thermo-Scientific, Waltham, MA, USA) by using coupled Zn/Se horizontal attenuated total reflectance (HATR) equipment. Films were laid on a clean crystal of the apparatus. The range of wavelength was 600 to 4000 cm^{-1} during the investigation. The spectra were obtained from 128 scans, at the spectral resolution of 4 cm^{-1} with CO_2 and H_2O for correction.

2.10. Raman spectroscopy

Raman spectroscopy is a widely used analytical method in pharmaceutical technology. In this article, a Dispersive Raman spectrometer was applied to confirm the relatively uniform distribution of the API in free polymer films. Transmission Raman Spectroscopy is used for non-invasive and fast qualitative investigation of pharmaceutical dosage forms and intermediate products. In our method, the distribution of PR was analyzed by Raman surface mapping. Our further aim was to search for possible interactions between the components of the films.

To investigate the distribution of the API, Raman spectra were acquired with a Thermo Fisher DXR Dispersive Raman (Thermo Fisher Sco. Inc., Waltham, MA, USA) equipped with a CCD camera and a diode laser operating at a wavelength of 780 nm. Raman measurements were carried out with a laser power of 24 mW at a slit aperture size of 25 μm on a spot size of 2 μm. The discrete spectra of the individual substances such as PR, HPMC and SA as well as different compositions of polymer films were collected with an exposure time of 6 s, and the number of exposures was 20. Smart background was used during the whole investigation. The applied spectral range was 3200–200 cm^{-1} with cosmic ray and fluorescence corrections.

2.11. Cell viability test

The cytotoxicity of PR films was studied on a Guava® easyCyte™ 5HT (Luminex, Austin, TX, USA) flow cytometer. The suspension of TR-146 cells in 1×10^6 million cells per mL concentration was treated with 1 mL of PR solution for half an hour (PR films were dissolved in HBSS in the same concentration as in the case of the permeation tests). After incubation, the sample solutions were removed, and the cells were washed twice with HBSS. After centrifuging the cells and removing the washing solution, with fresh HBSS, the original concentration of the suspension was restored and 1 μL of 100 μg/mL propidium iodide solution was added to each sample. After 15 min of staining, the cell suspensions were distributed on 96-well microplates in a volume of 200 μL (3 wells/group) and analyzed. Propidium iodide was excited with a 488 nm laser and detected at the 525/30 nm channel (green parameter). On the FSC-SSC scatterplot, the non-cellular events were excluded. The remaining events (8000–10,000) were analyzed on a scatterplot, and gates were created to determine stained (necrotic) and non-stained (living) cells. The experiment was carried out in duplicates.

2.12. Permeation test

The permeation of the API was measured on the TR146 buccal cell line under in vitro conditions.

2.12.1. Cell culturing

TR-146 cells (ECACC No: 10,032,305) were cultured in Dulbecco's modified Eagle's medium with 0.584 g/L L-glutamine and 4.5 g/L D-glucose. The cell culturing medium was supplemented with 10% (v/v) FBS, 3.7 g/L sodium hydrogencarbonate, 1% (v/v) non-essential amino acid solution, and 100 IU/mL penicillin K, with 100 μg/mL streptomycin sulphate. The cells were kept at 37 °C in 5% CO_2 containing atmosphere. The cells used for our experiments were between passage numbers 24 and 34.

2.12.2. In vitro permeation test

1×10^5 cells were seeded on ThinCert® PET cell culture inserts (0.4 μm pore size, $2 \times 10^6/cm^2$ pore density, 33.6 mm^2 culturing surface; Greiner BioOne, Mosonmagyaróvár, Hungary). Fresh culture medium was added to the cells every 4 days and 16 days passed between the seeding and the permeation experiments. A Millicell ERS 1 device was used to measure transepithelial electrical resistance (Merck, Budapest, Hungary). Only inserts with a resistance value over 130 Ω*cm^2 were used for the permeation tests. Films were cut to equal weight with a size of 28.26 mm^2 and dissolved in Hank's balanced salt solution (HBSS) in a concentration of 0.85 mg/mL before the experiment. First, the cell culture medium was removed and 400 μL of the dissolved films was added to the apical compartment (AC) and 1000 μL of HBSS to the basolateral compartment (BC) of each selected insert. 200 μL of HBSS was removed from the BC after every 30 min and the removed volume was replaced with fresh solvent. The samples were placed into low UV absorbance 96-well plates (UV-Star, Greiner BioOne, Mosonmagyaróvár, Hungary) and their absorbance was measured at 261 nm with a Multiskan Go microplate reader (Thermo-Fisher, Waltham, MA, USA). Apparent permeability (P_{app}) was calculated as: $(\Delta Q/\Delta t)*(1/(0.336\ cm^2*C_0))$, where C_0 is the concentration of the tested compound (mol/mL); $\Delta Q/\Delta t$ is the rate of permeability of the tested compound (mol/s). The calculation was made for the time intervals of 0–30, 30–60 and 60–90.

2.13. Statistical analysis

The significance tests for breaking hardness and in vitro mucoadhesivity were performed with Microsoft Excel (version 15, Redmond, Washington, DC, USA) software. A two-sample *t*-test was used. The test was done six times for each sample. The average values of apparent permeability were calculated from the apparent permeability measured between 0 and 30, 30–60 and 60–90 min. After that, a Kruskal-Wallis test with Dunn's test as a post hoc test was performed to compare the averages. Calculations were carried out by GraphPad Prism software (version 8, GraphPad Software, San Diego, CA, USA). In all cases, the samples were compared to Sample 1. In each case, we used a significance level of $p < 0.05$. Significance is labelled as ns = $p \geq 0.05$; * = $p < 0.05$.

3. Results and discussion

3.1. Thickness of films

It is very important to investigate the thickness of the buccal films in terms of patient compliance, releasing process of the drug and applicability of the dosage form. Polymer films should be thin because it can cause discomfort to the patient if they are too thick. On the other hand, the thickness of the films influences the kinetics of drug release from the films. In the case of thin films, the API dissolved fast, but from thick films the API release is slower because it needs more time to wet and dissolve. During the application, the patient presses the film to the buccal mucosa

Table 2
Thickness and water content of the films ($n = 8$).

Samples	Thickness (μm) ± SD	Water content (%) ± SD
1	59.62 ± 3.05	7.63 ± 0.23
2	80.85 ± 2.68	9.12 ± 0.64
3	77.81 ± 3.35	9.88 ± 0.91
4	67.03 ± 3.39	7.44 ± 0.77
5	83.42 ± 1.82	9.68 ± 1.06
6	91.47 ± 4.93	10.78 ± 0.58
7	72.64 ± 6.88	8.93 ± 1.24
8	78.88 ± 4.49	9.72 ± 1.65
9	107.49 ± 5.59	11.55 ± 0.71

and if it is too thin, it can break easily, so it is unapplicable.

Table 2. shows the results of the thickness and the moisture content measurement of the different polymer film compositions. As can be seen, the thinnest film is the one with lower SA and GLY content (Sample 1) and it contains the least amount of water. In the films containing a higher SA concentration, the thickness of the prepared films can be increased, so the concentration of SA can influence the thickness of the films. However, GLY also has an effect on the thickness of the prepared films. GLY has a water retention effect, so films with a higher GLY content are thicker because they contain more water in the polymer film system (Gao et al., 2019; Pamlényi et al., 2021) as it can be seen in Table 2. It can be stated that GLY can increase the thickness of films. On the other hand, in the case of our films it can be seen that films with a higher GLY concentration contain more residual water than films with a lower GLY concentration, so GLY can affect water retention in the films, as confirmed by the measurement. Overall, it is important to investigate the thickness of the films because if they are very thick, they can reduce patient compliance, furthermore, the dissolution of the API can also be slow because the API has to go through a thick layer and needs more time to release. According to the literature, the formulated films have sufficient thickness to be applied on the buccal mucosa (El-Maghraby and Abdelzaher, 2015)."

3.2. Breaking hardness of films

Fig. 2. shows the results of the breaking hardness measurements. The buccal film is an innovative dosage form. In the literature, there is no standard measurement, similarly to nanotechnology, or an accurate, accepted limit for the tensile strength of a buccal film to be applied on the buccal mucosa. We tried to simulate the application force to the mucosa with finger. The moving part of our equipment was removed and the film was pressed with finger, with a force similar to what the patients

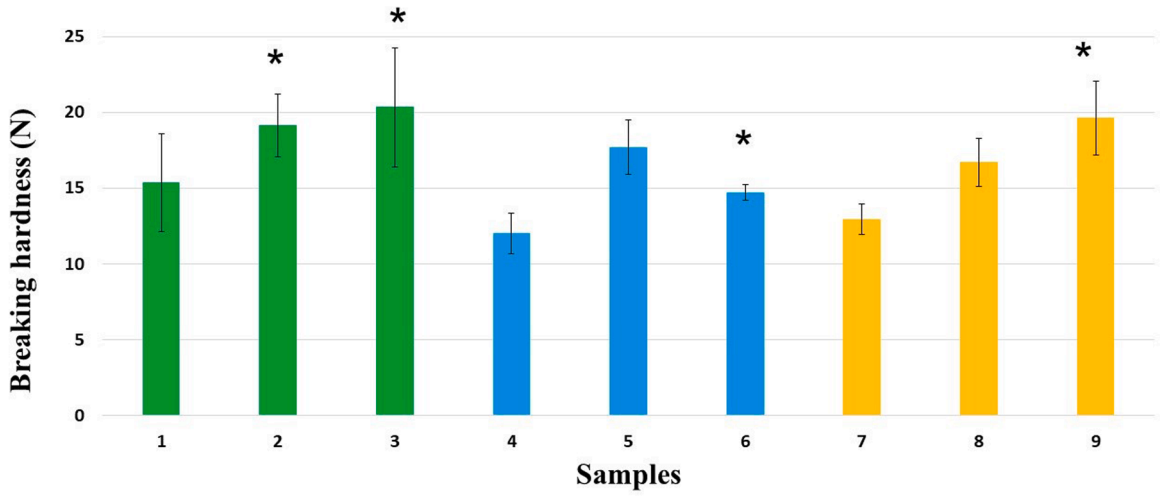

Fig. 2. Tensile strength of the prepared films (* $p < 0.05$; $n = 8$). (For interpretation of the references to color in this figure legend, the reader is referred to the web version of this article.)

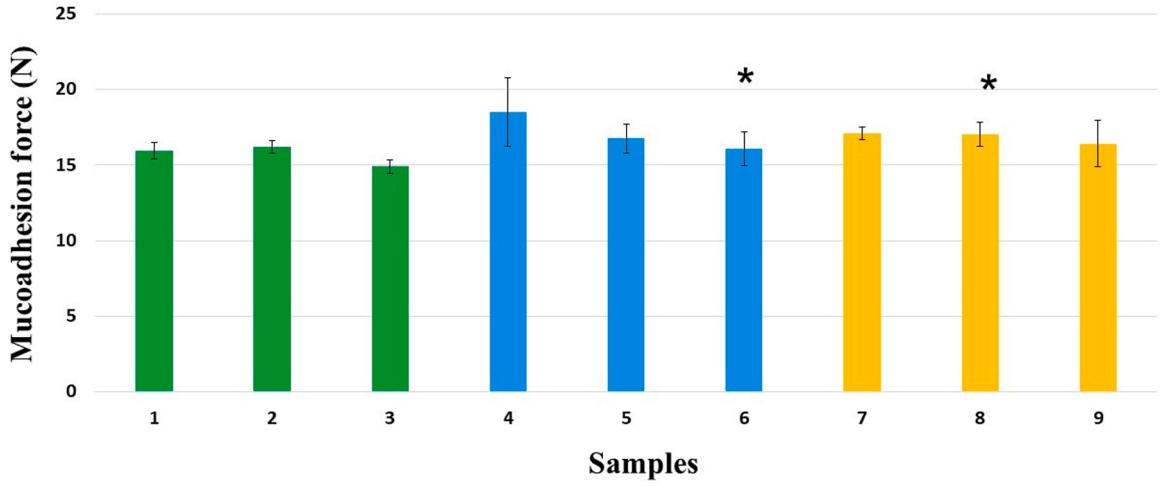

Fig. 3. Mucoadhesion force of the polymer films of different compositions (* $p < 0.05$; $n = 8$). (For interpretation of the references to color in this figure legend, the reader is referred to the web version of this article.)

Table 3
CA, SFE its dispersive (γ^d) and polar part (γ^d) and polarity (%) of the prepared films ($n = 5$).

Samples	CA (°) water	CA (°) diiodomethane	γ^{total} (mN/m)	γ^d (mN/m)	γ^p (mN/m)	Polarity (%)
1	54.94 ± 5.53	43.09 ± 2.99	56.03	34.70	21.33	38.07
2	54.01 ± 3.27	45.68 ± 4.19	45.79	33.82	11.98	26.16
3	68.84 ± 4.90	46.61 ± 0.66	47.89	33.29	14.6	30.49
4	59.03 ± 2.73	52.04 ± 1.51	46.00	30.77	15.23	33.11
5	53.22 ± 3.63	43.78 ± 1.09	56.72	34.38	22.34	39.39
6	56.79 ± 1.99	47.81 ± 0.47	53.62	32.59	21.13	39.41
7	52.74 ± 3.73	47.88 ± 3.33	55.76	32.52	23.24	41.68
8	71.54 ± 2.51	48.64 ± 1.41	45.92	32.40	13.52	29.44
9	76.48 ± 2.50	41.76 ± 1.07	46.07	35.66	10.41	22.60

would apply to press it to the mucosa.

As can be seen in Fig. 2., the films with higher GLY concentration have a higher breaking hardness value, so these films are more flexible because of the plasticizer properties of GLY. Besides, these films are more resistant to pressure due to their greater thickness because of the larger water content and the H-bonding between GLY and the film forming agents. On the other hand, when increasing the amount of SA in the composition of the polymer films, it can be observed that the breaking hardness of films can be reduced. The difference between the 1:2 ratio SA and HPMC, equal amounts of the two polymers and 2:1 ratio SA and HPMC is less than 2–3 N and not significant.

We concluded that a force of 10 N is sufficient to create mucoadhesion to the buccal mucosa (Pamlényi et al., 2021). So films must have a tensile strength greater than 10 N to be applicable appropriately.

All film compositions have a breaking hardness higher than 10 N, for the composition with the worst result (Sample 4) it is higher than 12 N, so it can be said that with respect to breaking hardness properties, every composition is suitable for application on the buccal mucosa.

3.3. *In vitro mucoadhesivity of films*

At the beginning of our project, we formulated films from SA without other excipients (for example, plasticizer, API) (Pamlényi et al., 2022, 2021). The prepared films were examined with different methods, including in vitro mucoadhesivity. The mucoadhesivity data revealed that the films with 2% SA concentration have 7.44 $N \pm 0.23$ N, while for the films with 3% SA concentration this value is close to 20 N with our equipment. From the literature we know that SA has smaller mucoadhesivity (with our equipment more than 7 N) than cellulose derivatives, but its mucoadhesivity is also enough to bind to the buccal mucosa (Kesavan, 2010). We drew the limit at 7 N. So, if the mucoadhesivity of the different compositions is greater than 7 N, it means they have sufficient mucoadhesion force to bind to the buccal mucosa (Pamlényi et al., 2022, 2021) . In this project, we formulated just 3% polymer films.

Fig. 3. shows the results of the in vitro mucoadhesivity test. As can be seen, every composition has great and adequate mucoadhesivity properties, larger than 7 N. The in vitro mucoadhesion force of all samples is higher than 15 N. The ratio of the polymer types has a negligible influence on the mucoadhesivity of the films. It can be stated that films with a lower SA ratio (Samples 1–3) have similar mucoadhesion values as films with a higher SA ratio (Samples 7–9). The mucoadhesion values of films which have equal amounts of the two polymers (Samples 4–6) are slightly higher, but there is no significant difference. In our previous work, it was concluded that the GLY concentration can reduce the mucoadhesion force of films due to the phenomenon that hydrogen bonding can be created between GLY and the polymer film forming agents, and due to this interaction, fewer free chains remain in the polymer film system which could bind to the chains of mucin on the buccal mucosa (Pamlényi et al., 2021). This observation can also be valid, but the differences between the different compositions are not remarkable. It can be seen that GLY decreases the mucoadhesivity of films, so films containing a higher amount of GLY have smaller in vitro mucoadhesivity than films with a lower GLY concentration. Overall, SA can enhance the force of mucoadhesion, especially in the case of equal amounts of the two polymers (Samples 4–6), so in these cases SA can form stronger binding to the mucin due to its free carboxylic and hydroxylic groups. It can be said that SA can be used as a film forming agent in a buccal drug delivery system due to this in vitro mucoadhesivity property.

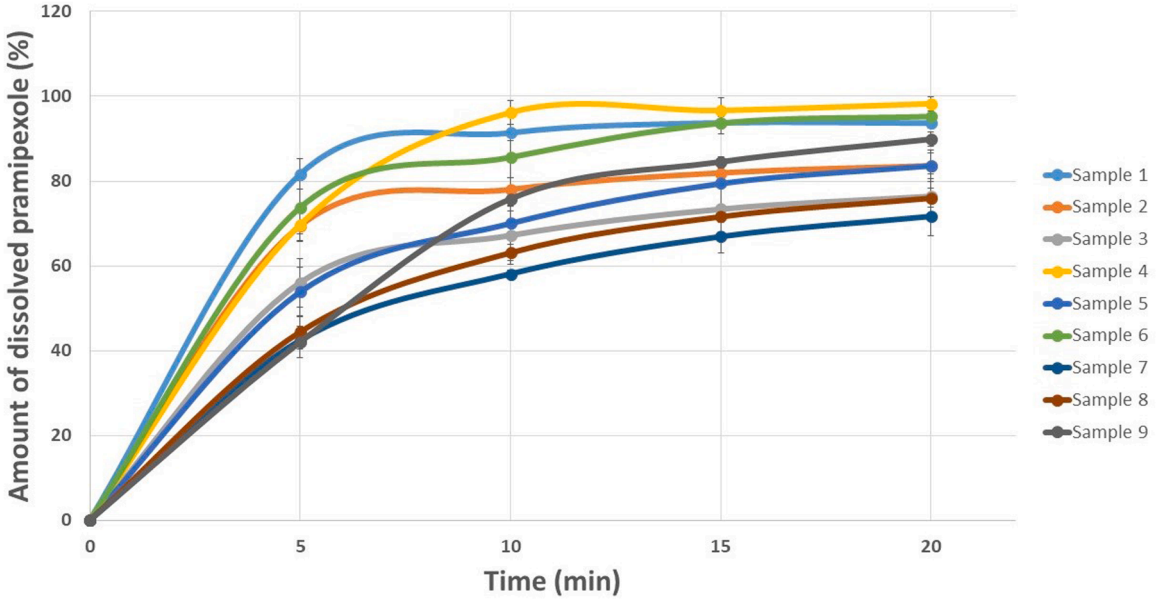

Fig. 4. Dissolution of PR from the different polymer films under 20 min ($n = 6$). (For interpretation of the references to color in this figure legend, the reader is referred to the web version of this article.)

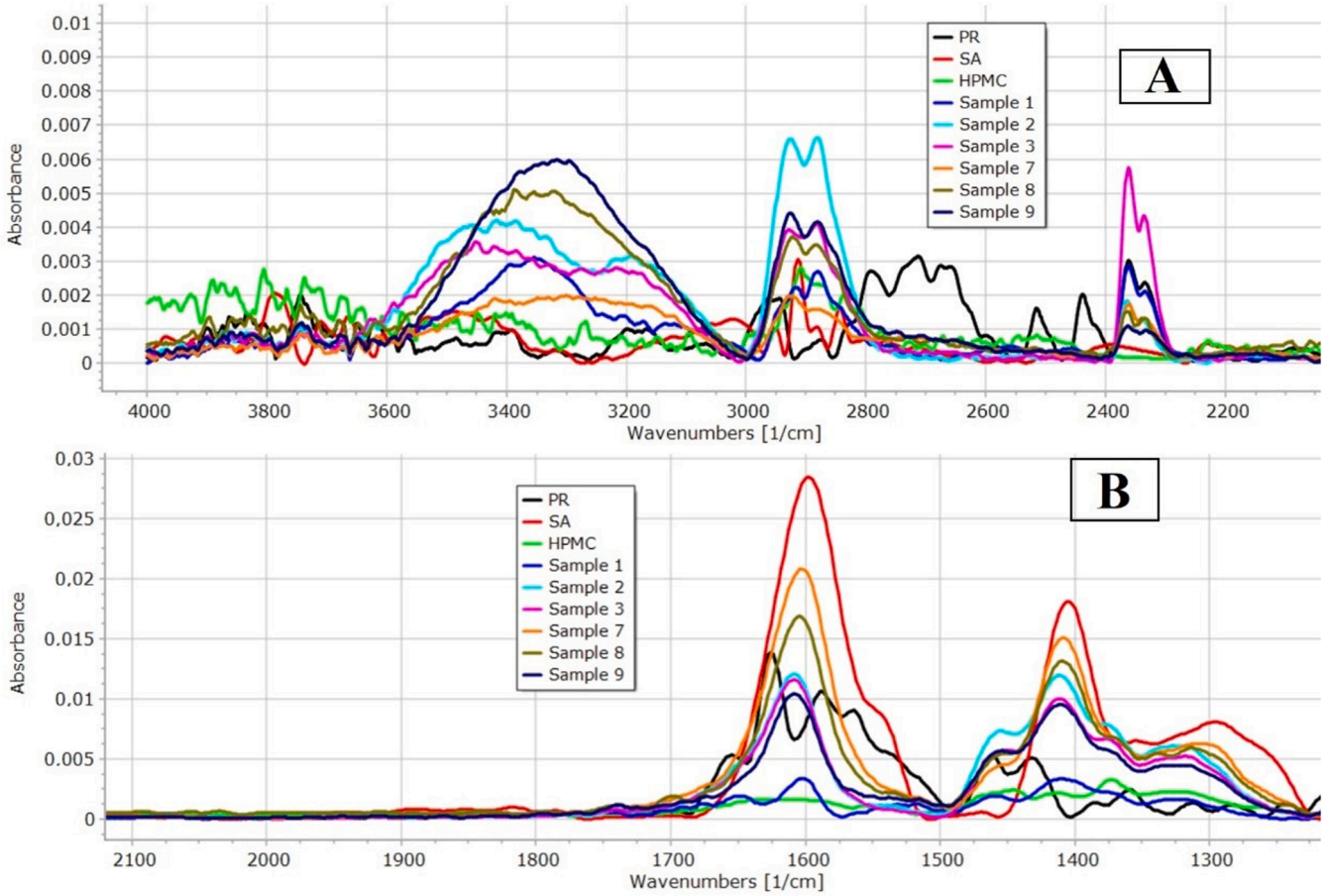

Fig. 5. FT-IR spectra of the prepared films (Part „A" from 4000 cm^{-1} to 2100 cm^{-1}, Part „B" from 2200 cm^{-1} to 1200 cm^{-1}). (For interpretation of the references to color in this figure legend, the reader is referred to the web version of this article.)

3.4. Contact angle measurement and surface free energy (SFE)

The surface free energy (SFE) and the polar and disperse components of the ingredients and the films were calculated from the measured contact angle. The disperse part was from the London dispersion force, while the polar part was from dipole-dipole interaction, induction force, and H-bonds. The CA and SFEs of the different samples can be seen in Table 3. This study is very important from the aspect of applying this dosage form because the saliva should spread extensively on the film surface for mucoadhesion to develop between the chains of the mucin and the chains of the film. As can be seen in Table 3., the polymer type cannot significantly influence CA in the case of water and diiodomethane. GLY can affect the surface properties, it can increase CA, so films with a lower GLY concentration have a lower CA value, which means that water or saliva can spread better on the surface of these films than in the case of using higher GLY concentrations. The SFE values are between 45 mN/m and 57mN/m. Our results show that the data correlate with the literature data, they are somewhat lower (Gottnek et al., 2013). There is no correlation between the polymer type and SFEs, nevertheless, the films with the lowest GLY content (Sample 1, Sample 4, Sample 7) have the highest SFE values.

Overall, it can be said that the contact angle (CA) of the liquid dropped onto the surface of the films with the lowest GLY content is the smallest, which means the saliva can spread on the surface of the buccal mucosa to a greater extent, so they have appropriate surface properties. They also have a high SFE value, and they have the highest polarity (Sample 1 - 38.07% and Sample 7 - 41.68%). Overall, on these surfaces, CA is small, which promotes proper spreading of the salvia on the surface, and the SFE is relatively large, which promotes the adhesion of proteins (e.g., mucin) (Falde et al., 2016; Sterzenbach et al., 2020).

3.5. Dissolution test

The API has to be released fast from buccal films because the buccal film cannot stay on the buccal mucosa for a long time as the saliva moistens it and detaches it from the surface. Therefore, the API must dissolve from the film earlier than the film separates from the buccal mucosa. Fig. 4. shows the results of the dissolution studies. As can be seen, from most of the compositions more than 80% PR can be dissolved under 20 min, and the release of PR is higher from Sample 1, Sample 4 and Sample 6 in the first 10 min. The type of the polymer can influence the drug release rate because from the films with a higher (2%) SA content, the API is dissolved more slowly (Sample 7, Sample 8, Sample 9), so it can be stated that SA can slow down the release of the API. However, drug release is faster from the films with a higher HPMC concentration or equal amounts of the two polymers, as can be seen in Fig. 4. This phenomenon can be explained by the viscosity of the films. Films with a higher SA concentration can wet and swell by the dissolution media, and the viscosity of these films is higher, therefore the release of the API can be slower. The viscosity of films with a higher HPMC content is lower and the dissolution of API is faster.

However, the plasticizer also has an effect on dissolution. The films with the lowest GLY content, Sample 1 and Sample 4, can release the API faster than the films with 2% and 3% GLY concentration, except for Sample 6. As can be observed, the API is dissolved from the film with a low GLY content at the highest rate from 5 min onwards. This effect is not perceptible in the case of Sample 7, since that sample contains a high SA concentration, so the high SA content can decrease drug release and

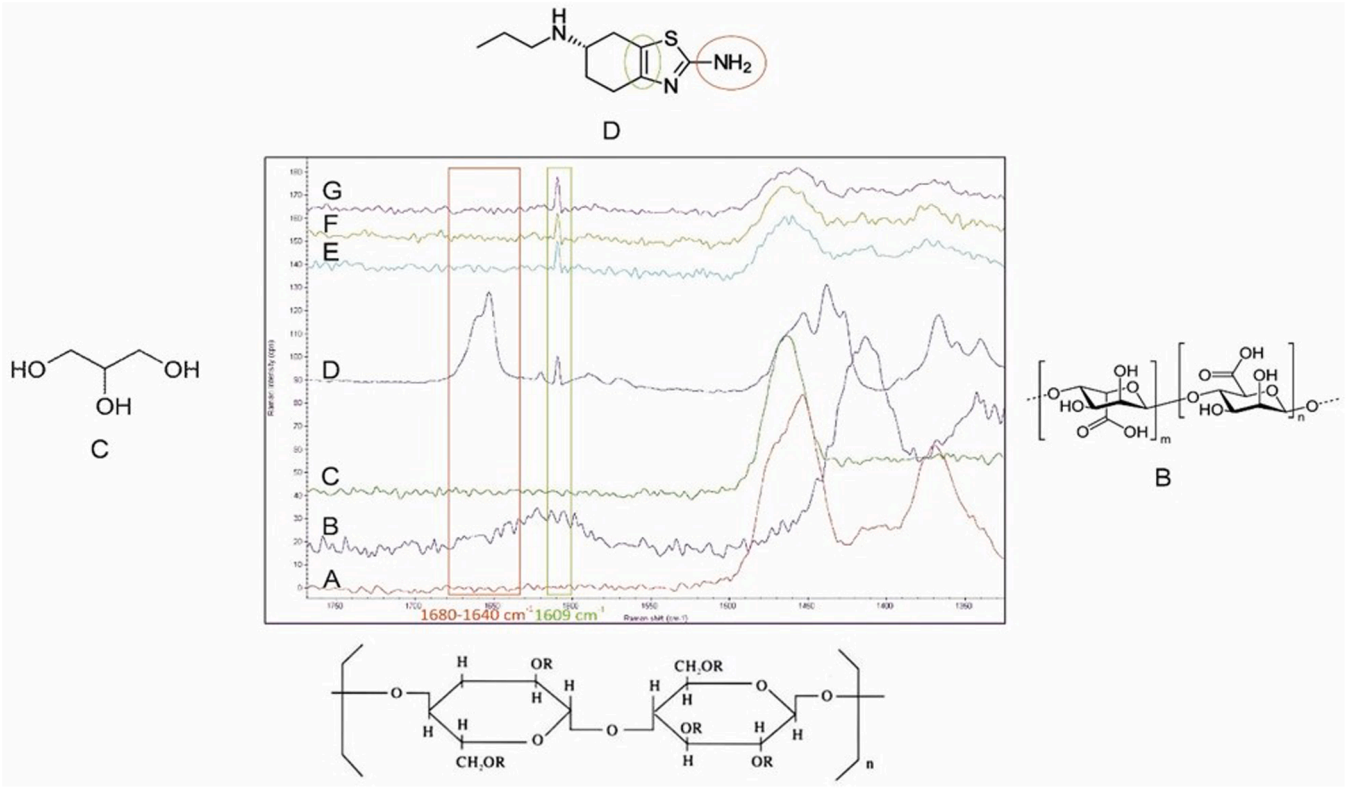

Fig. 6. **A**: the chemical structure and the spectrum of HPMC; **B**: the chemical structure and the spectrum of SA; **C**: the chemical structure and the spectrum of GLY; **D**: the chemical structure and the spectrum of PR; **E**: the spectrum of buccal film with 3% GLY content; **F**: the spectrum of buccal film with 2% GLY content; **G**: the spectrum of buccal film with 1% GLY content. Rounding with orange: The peak of PR at 1680–1640 cm^{-1} represents the vibration of the primary amine group, which cannot be recognized in the polymer films. Rounding with green: The persistence of the peak of PR at 1609 cm^{-1} represents the vibration of C═C conjugated with the aryl group. (For interpretation of the references to color in this figure legend, the reader is referred to the web version of this article.)

offset the expected result.

At the same time, it can be stated that by the end of the dissolution test (120 min), the whole amount of the API can be dissolved from each composition.

Finally, it can be concluded from the results of the dissolution test that the fast-releasing films Sample 1, Sample 4 and Sample 6 can be recommended for further development and use in Parkinson's disease as a buccal polymer film dosage form.

3.6. FT-IR spectroscopy

Fig. 5. shows the FT-IR spectra of the raw materials and the different compositions of films. In part „A" of Fig. 5., at 2305 cm^{-1}, a sharp peak can be seen, which is related to the C—S═N band of the thiazole group. This peak can also be observed sharply in all samples, which proves that the API can be found in the films without significant chemical change.

In the higher wavenumber region, from 2922 cm^{-1} to 2852 cm^{-1} stretching vibration of aliphatic C—H groups of PR, GLY, HPMC and SA can be explored in the spectra of the raw materials (Limoee et al., 2022). As can be seen in the spectra of the samples, the individual peaks of the raw materials overlapped with each other due to the different stretching vibration of C—H groups which can be found in the polymer film system from the different components, which means that interactions and connections can be formed between the components of the films, which can be observed in the spectra of all samples as a double peak. The double peak can also show that new chemical bonds can be created between the C—H group of PR and SA.

At 3197 cm^{-1} and 3394 cm^{-1} the N—H stretching vibration can be seen in the spectra of PR (Muthu et al., 2013). A spectral peak can be explored at 3310 cm^{-1}, which corresponds to the stretching vibration of the O—H group of GLY (Pamlényi et al., 2021; Tzankov et al., 2019). In this region, there is a wide peak in the spectra of the different samples, which is created by the interaction between the N—H group of PR, the O—H group GLY, SA and HPMC. The peak shifts to the higher wavenumber due to the higher amount of HPMC, so it can be stated that intermolecular H-bonds can be created between the components of the films.

In part „B" of Fig. 5., at 1410 cm^{-1}, a sharp peak can be observed in the polymer films. This peak is related to the symmetrical stretching of the COO^- groups in SA. In addition, at 1427 cm^{-1} wavenumber C—N stretching vibration of PR is manifested, but in the polymer film this peak totally disappears, which shows an interaction between the components of the films (Muthu et al., 2013).

Two peaks appeared at 1637 cm^{-1} and at 1582 cm^{-1} related to the stretching vibration of C═N and C═C in the spectrum of PR, respectively (Limoee et al., 2022). At the same time, at 1595 cm^{-1} a large sharp peak is also manifested, which is the asymmetrical stretching vibration of COO^-. As can be seen in the samples, the two peaks of PR totally disappeared and obscured the peak of SA. On the other hand, the peak of SA was shifted to the higher wavenumber. The degree of the shift correlates with the concentration of SA, and the shift can be considered as a sign of interaction between SA and PR.

3.7. Raman spectroscopy

In this investigation process, we analyzed the individual spectra of film components and the polymer films with different compositions of additives. Chemical mapping was used to analyse the distribution of PR in the films. The main findings of the spectra were the following:

- the disappearance of a peak at 1680–1640 cm^{-1} in all free films,

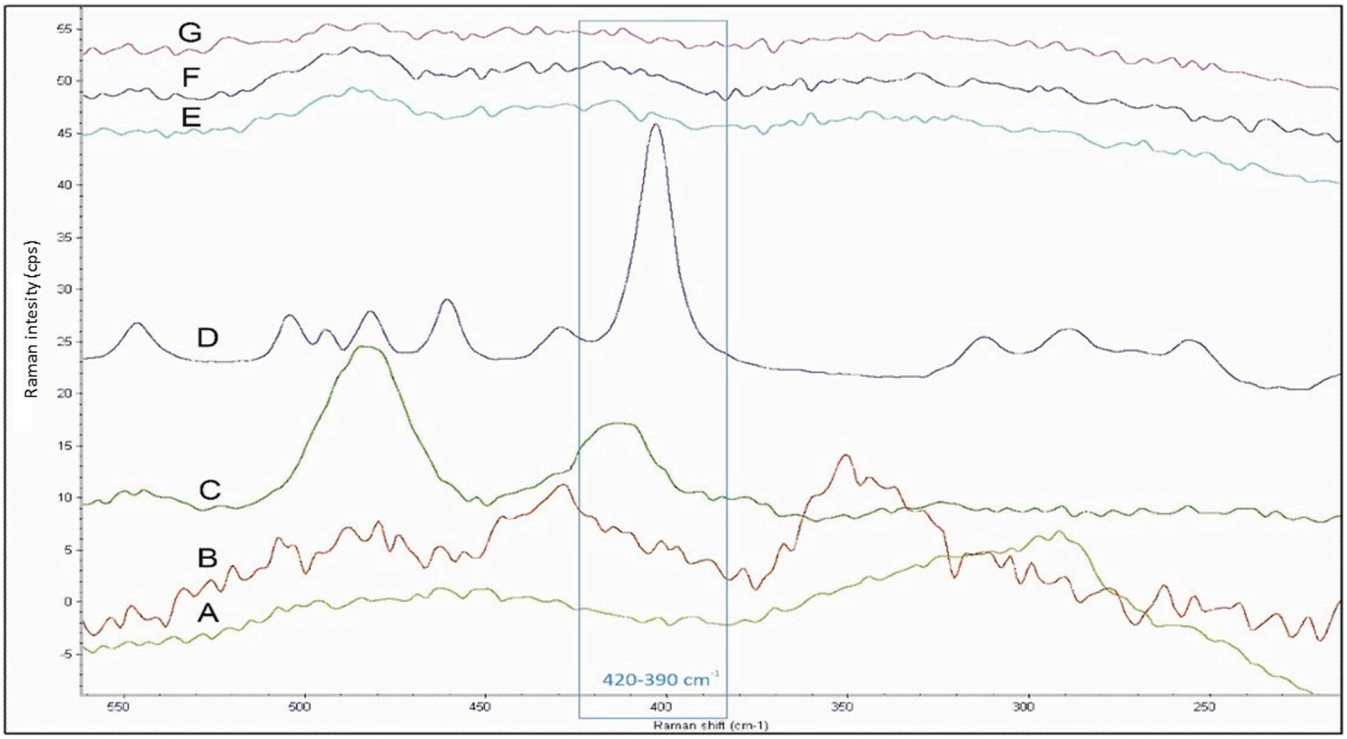

Fig. 7. **A**: The spectrum of HPMC; **B**: the spectrum of SA; **C**: the spectrum of GLY; **D**: the chemical structure and the spectrum of PR; **E**: the spectrum of buccal film with 3% GLY content; **F**: the spectrum of buccal film with 2% GLY content; **G**: the spectrum of buccal film with 1% GLY content. Rounding with blue: The disappearance of the peak at 420–390 cm^{-1} assigned as the amine group (primary aliphatic amines) in the buccal films. (For interpretation of the references to color in this figure legend, the reader is referred to the web version of this article.)

- the persistence of the detectability of the peak at 1609 cm^{-1} in all free films,
- the disappearance of a peak at 420–390 cm^{-1} in all free films."

These regions of the spectra were assigned. The peak of PR at 1680–1640 cm^{-1} represents the vibration of the primary amine group, which cannot be recognized in the polymer films at all (Fig. 6.). The peak at 420–390 cm^{-1} was also assigned as the amine group (primary aliphatic amines), which also disappeared in the spectra of the films (Fig. 7.). The disappearance of these two peaks means an interaction of PR with the other components. Due to the chemical structure of the components, it is possible between the –NH2 group of PR and the –OH groups of GLY, SA and HPMC. It can therefore be stated that intermolecular H-bonds can be created between the components, as was also established by the FT-IR measurement.

The peak of PR at 1609 cm^{-1} represents the vibration of C═C conjugated with the aryl group. This vibration is visible in all polymer films regardless of the GLY concentration. In the chemical structure of the components, C═C bonding is present only in the structure of the API (Fig. 6.). The persistence of this peak indicates the presence of PR. So the distribution of the API was profiled with this selected peak. Fig. 8. (chemical map) shows the completely homogeneous distribution of PR in the films.

3.8. Biocompatibility test

The TR-146 cells were treated with the dissolved films in the concentration of 0.85 mg/mL PR in HBSS as a solvent. Table 4. shows the results of the cytotoxicity test according to flow cytometry. It can be seen that the formulations had very little impact upon the cell viability of the cells. As such, all films can be considered nontoxic.

3.9. In vitro permeation test

The cellular permeation of pramipexole was studied on TR-146 for 90 min with 3 sampling times and with the same concentration as in the case of the cell viability test. The apparent permeability was calculated for each 0–30, 30–60 and 60–90 min and the average of these values were plotted in Fig. 8. The films were previously fully dissolved in HBSS. As shown in Fig. 9., Samples 1, 3, 7, 8 and 9 had approximately similar permeability. Samples 2, 4 and 5 had higher permeation, while Sample 6 had the lowest permeability.

Most films had a stable rate of permeation throughout the experiment (Fig. 10.). The only notable exception is Sample 5, which had a greatly increased amount of permeated PR between 30 and 60 min, and Sample 9, which had a decreased speed after 60 min. For the other samples, it can be said that the release of PR is continuous from the films without any dose dumping, making further applications safe for the patients. Overall, the excipients of the films did not obstruct the transcellular transport of the films, indicating a possibly high *in vivo* bioavailability.

4. Conclusion

One of the major difficulties in the treatment of Parkinson's disease is the difficulty in swallowing for the patients. The buccal mucoadhesive films produced in our work can solve this problem because the patients do not have to swallow the dosage form, and during application, pramipexole can be absorbed from the area of the buccal mucosa quickly without causing a foreign body sensation.

Our most important results are summarized below. The thickness of the films is determined by the type and the concentration of the polymer. At the same time, the concentration of the plasticizer can increase this parameter.

Films with a higher SA content have higher in vitro mucoadhesivity

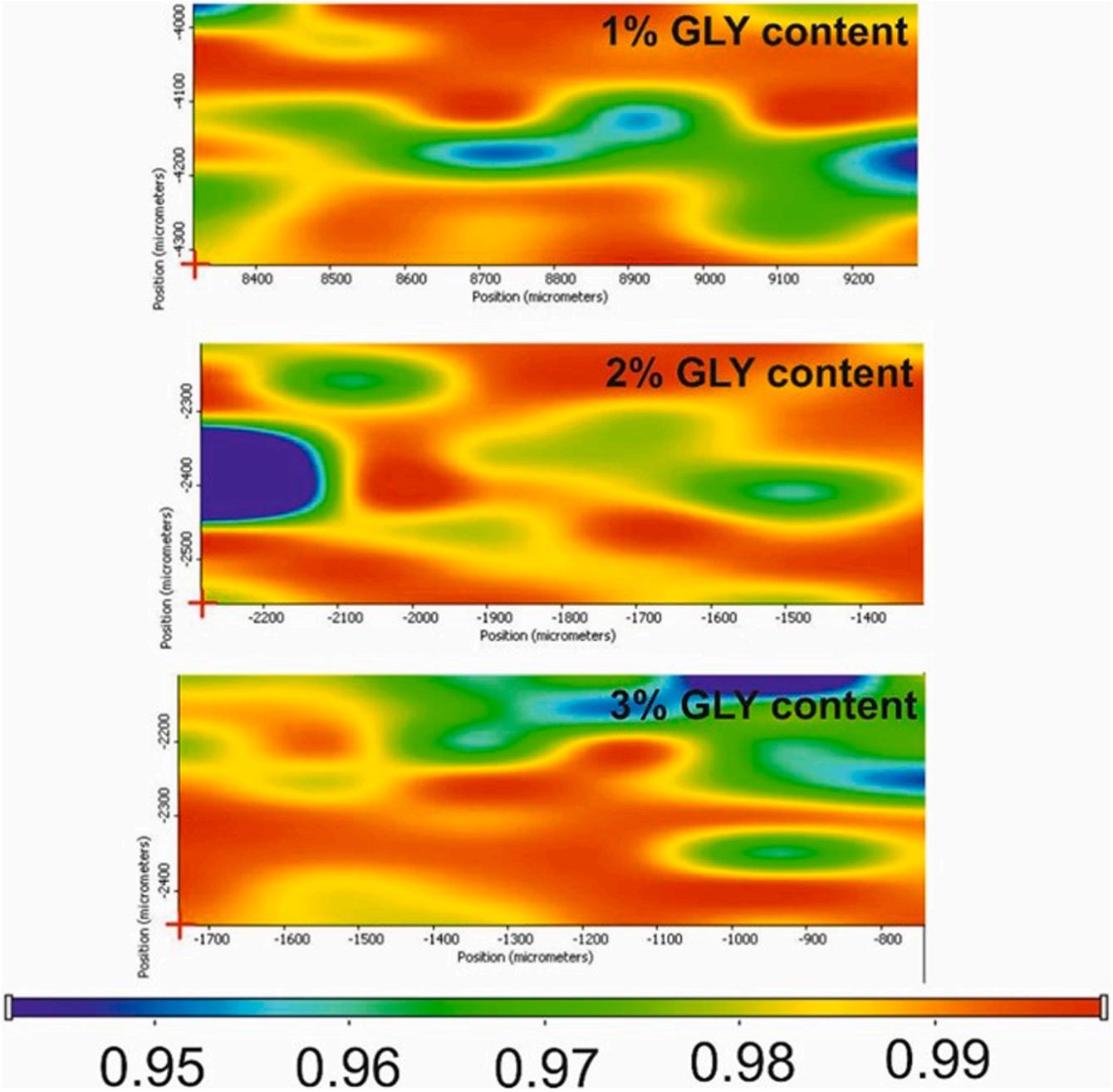

Fig. 8. Chemical maps of free films with different GLY content profiled with the peak of PR at 1609 cm^{-1} (vibration of C = C). The red colour suggests that the presence of the C = C bonding is more than 99%, while the blue colour suggests a presence of over 94–95%. So the colours show that the distribution of the API in the films is completely homogenous. (For interpretation of the references to color in this figure legend, the reader is referred to the web version of this article.)

values (Sample 7, Sample 8, Sample 9). On the other hand, GLY also has an effect on mucoadhesivity, it can decrease the binding between the polymer film and mucin. This is supported by the evaluation of the CA and SFE of different films, which reveals that the films with the lowest GLY concentration have the smallest CA and the highest SFE values, so the saliva can spread best on the surface of the film and can bind best to mucin. Therefore, it is recommended to apply a low concentration of GLY during formulation.

More than 80% of PR can be dissolved from the films in the first 20 min. From the promising compositions (Sample 1, Sample 2, Sample 4, Sample 6.), more than 70% of PR can be dissolved under 5 min so it allows comfortable application, without the feeling of a foreign body sensation during long application.

Interactions can be detected between the components of films in all samples. Intermolecular hydrogen bonds can be formed between the amino group of PR and the carboxylic group of SA, HPMC and GLY. This interaction of the film components causes assumed stability improvement in the free films. The API can be detected in the samples, so it can be said that the API does not undergo a chemical structure change therefore all the excipients can be used safely without reducing the effectiveness of PR.

Overall, the buccal films had negligible cytotoxicity and most of them had a constant rate of permeation through the TR-146 cell line layer.

Summarizing all the results, it can be said that Sample 1 and Sample 4 are recommended for application on the buccal mucosa. Based on our

Table 4
Cytotoxicity of the prepared films according to flow cytometry. The individual values of the samples are shown as the percentage of the cell viability of the untreated control cells.

Samples	Cell viability% ± SEM
1	95.7 ± 1.31
2	95.0 ± 0.45
3	100 ± 0.57
4	100 ± 0.74
5	100 ± 0.11
6	100 ± 0.31
7	100 ± 1.24
8	87.1 ± 0.21
9	92.3 ± 0.45

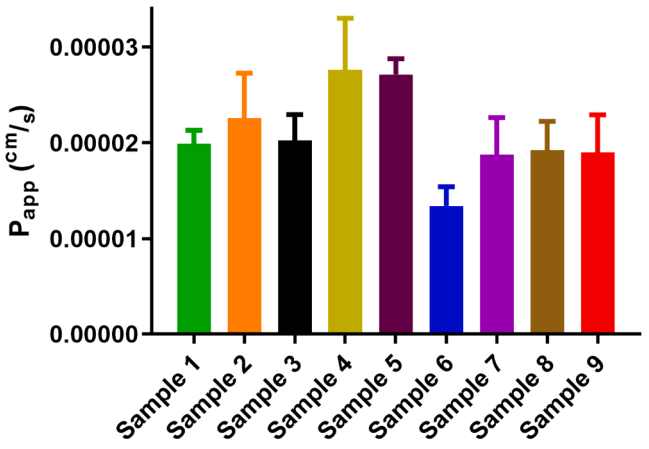

Fig. 9. Average (±SEM) apparent permeability of buccal films calculated from the permeability rate of PR between 0 and 30, 30–60 and 60–90 min. Each film was investigated in three separate, parallel cell culture inserts. No significant difference was found between the samples. (For interpretation of the references to color in this figure legend, the reader is referred to the web version of this article.)

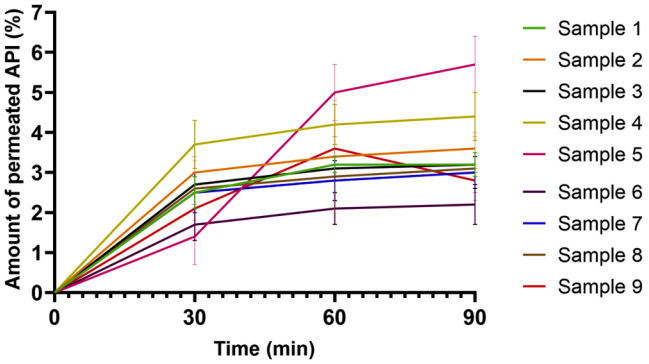

Fig. 10. Transported PR-time curves of buccal films on TR-146 cells. Each point represents the average of three separate, parallel cell culture inserts ± SEM. The amount of the permeated API was compared to the initial concentration of the dissolved film in the apical chamber. (For interpretation of the references to color in this figure legend, the reader is referred to the web version of this article.)

results, these samples are the ones that can be used to implement a more comfortable and better patient compliance therapy for Parkinson's disease patients.

Funding

The publication was funded by The University of Szeged Open Access Fund (FundRef, Grant No. 5991). This research work was supported by Richter Gedeon Talentum Foundation to help me participate in the PhD program (Grant No. 100822). This work was also supported by the New National Excellence Program of the Ministry for Innovation and Technology from the Source of the National Research, Development and Innovation Fund (Grant No. ÚNKP-21-3).

Conflicts of interests

The authors declare that they have no conflicts of interest.

CRediT authorship contribution statement

Krisztián Pamlényi: Methodology, Investigation, Formal analysis, Data curation, Visualization, Funding acquisition, Writing – original draft, Writing – review & editing. **Géza Regdon:** Conceptualization, Resources, Supervision, Funding acquisition, Project administration, Writing – original draft, Writing – review & editing. **Orsolya Jójárt-Laczkovich:** Data curation, Formal analysis, Writing – original draft. **Dániel Nemes:** Methodology, Investigation, Data curation, Formal analysis, Writing – original draft. **Ildikó Bácskay:** Formal analysis, Writing – original draft, Writing – review & editing. **Katalin Kristó:** Conceptualization, Supervision, Project administration, Data curation, Writing – original draft, Writing – review & editing.

Acknowledgements

The authors thank Krka, d. d., Novo mesto, Slovenia for supplying pramipexole dihydrochloride.

References

Aarsland, D., Creese, B., Politis, M., Chaudhuri, K.R., ffytche, D.H., Weintraub, D., Ballard, C., 2017. Cognitive decline in Parkinson disease. Nat. Rev. Neurol. 13, 217–231. https://doi.org/10.1038/nrneurol.2017.27.

Allen, R.P., Chen, C., Garcia-Borreguero, D., Polo, O., DuBrava, S., Miceli, J., Knapp, L., Winkelman, J.W., 2014. Comparison of pregabalin with pramipexole for restless legs syndrome. N. Engl. J. Med. 370, 621–631. https://doi.org/10.1056/NEJMoa1303646.

Alves, T.F.R., Rios, A.C., da Silva Pontes, K., Portella, D.L., Aranha, N., Severino, P., Souto, E.B., Gonsalves, J.K.M., de Souza Nunes, R., Chaud, M.V., 2020. Bilayer mucoadhesive buccal film for mucosal ulcers treatment: development, characterization, and single study case. Pharmaceutics 12, 657. https://doi.org/10.3390/pharmaceutics12070657.

Antonini, A., Tolosa, E., Mizuno, Y., Yamamoto, M., Poewe, W.H., 2009. A reassessment of risks and benefits of dopamine agonists in Parkinson's disease. Lancet Neurol. 8, 929–937. https://doi.org/10.1016/S1474-4422(09)70225-X.

Balestrino, R., Schapira, A.H.V., 2020. Parkinson disease. Eur. J. Neurol. 27, 27–42. https://doi.org/10.1111/ene.14108.

Barrett, M.J., Sargent, L., Nawaz, H., Weintraub, D., Price, E.T., Willis, A.W., 2021. Antimuscarinic anticholinergic medications in Parkinson disease: to prescribe or deprescribe? Mov. Disord. Clin. Pract. 8, 1181–1188. https://doi.org/10.1002/mdc3.13347.

Boateng, J., 2017. Drug delivery innovations to address global health challenges for pediatric and geriatric populations (through improvements in patient compliance). J. Pharm. Sci. 106, 3188–3198. https://doi.org/10.1016/j.xphs.2017.07.009.

Chachlioutaki, K., Tzimtzimis, E.K., Tzetzis, D., Chang, M.-W., Ahmad, Z., Karavasili, C., Fatouros, D.G., 2020. Electrospun orodispersible films of isoniazid for pediatric tuberculosis treatment. Pharmaceutics 12, 470. https://doi.org/10.3390/pharmaceutics12050470.

de Souza Silva, M.A., Mattern, C., Häcker, R., Tomaz, C., Huston, J.P., Schwarting, R.K. W., 1997. Increased neostriatal dopamine activity after intraperitoneal or intranasal administration of L-DOPA: on the role of benserazide pretreatment. Synapse 27, 294–302. https://doi.org/10.1002/(SICI)1098-2396(199712)27:4<294::AID-SYN3>3.0.CO;2-7.

Diao, L., Shu, Y., Polli, J.E., 2010. Uptake of pramipexole by human organic cation transporters. Mol. Pharm. 7, 1342–1347. https://doi.org/10.1021/mp100036b.

El-Maghraby, G., Abdelzaher, M., 2015. Formulation and evaluation of simvastatin buccal film. J. App. Pharm. Sci. 070–077. https://doi.org/10.7324/JAPS.2015.50412.

Falde, E.J., Yohe, S.T., Colson, Y.L., Grinstaff, M.W., 2016. Superhydrophobic materials for biomedical applications. Biomaterials 104, 87–103. https://doi.org/10.1016/j.biomaterials.2016.06.050.

Fonseca-Santos, B., Chorilli, M., 2018. An overview of polymeric dosage forms in buccal drug delivery: state of art, design of formulations and their in vivo performance evaluation. Mater. Sci. Eng. 86, 129–143. https://doi.org/10.1016/j.msec.2017.12.022.

Gao, W., Liu, P., Li, X., Qiu, L., Hou, H., Cui, B., 2019. The co-plasticization effects of glycerol and small molecular sugars on starch-based nanocomposite films prepared by extrusion blowing. Int. J. Biol. Macromol. 133, 1175–1181. https://doi.org/10.1016/j.ijbiomac.2019.04.193.

Goberman, A.M., Blomgren, M., 2003. Parkinsonian speech disfluencies: effects of L-dopa-related fluctuations. J. Fluency Disord. 28, 55–70. https://doi.org/10.1016/S0094-730X(03)00005-6.

Gottnek, M., Süvegh, K., Pintye-Hódi, K., Regdon, G., 2013. Effects of excipients on the tensile strength, surface properties and free volume of Klucel® free films of pharmaceutical importance. Radiat. Phys. Chem. 89, 57–63. https://doi.org/10.1016/j.radphyschem.2013.04.017.

Hanif, M., Zaman, M., Chaurasiya, V., 2015. Polymers used in buccal film: a review. Des. Monomers Poly. 18, 105–111. https://doi.org/10.1080/15685551.2014.971389.

Hubsher, G., Haider, M., Okun, M.S., 2012. Amantadine: the journey from fighting flu to treating Parkinson disease. Neurology 78, 1096–1099. https://doi.org/10.1212/WNL.0b013e31824e8f0d.

Ibrahim, Y.H.-E.Y., Regdon, G., Kristó, K., Kelemen, A., Adam, M.E., Hamedelniel, E.I., Sovány, T., 2020. Design and characterization of chitosan/citrate films as carrier for oral macromolecule delivery. Eur. J. Pharm. Sci. 146, 105270 https://doi.org/10.1016/j.ejps.2020.105270.

Katzenschlager, R., Sampaio, C., Costa, J., Lees, A., 2002. Anticholinergics for symptomatic management of Parkinsonś disease. Cochrane Database Syst. Rev. 2010 https://doi.org/10.1002/14651858.CD003735.

Kelemen, A., Gottnek, M., Regdon, G., Pintye-Hódi, K., 2015. New equipment for measurement of the force of adhesion of mucoadhesive films. J. Adhes. Sci. Technol. 29, 1360–1367. https://doi.org/10.1080/01694243.2015.1029059.

Kelemen, A., Katona, B., Módra, S., Aigner, Z., Sebe, I., Pintye-Hódi, K., Zelkó, R., Regdon, G., Kristó, K., 2020. Effects of sucrose palmitate on the physico-chemical and mucoadhesive properties of buccal films. Molecules 25, 5248. https://doi.org/10.3390/molecules25225248.

Kesavan, K., 2010. Sodium alginate based mucoadhesive system for gatifloxacin and its in vitro antibacterial activity. Sci. Pharm. 78, 941–957. https://doi.org/10.3797/scipharm.1004-24.

Lee, A., Gilbert, R.M., 2016. Epidemiology of Parkinson disease. Neurol. Clin. 34, 955–965. https://doi.org/10.1016/j.ncl.2016.06.012.

Lemke, M.R., Brecht, H.M., Koester, J., Reichmann, H., 2006. Effects of the dopamine agonist pramipexole on depression, anhedonia and motor functioning in Parkinson's disease. J. Neurol. Sci. 248, 266–270. https://doi.org/10.1016/j.jns.2006.05.024.

Limoee, M., Allahdad, M., Samadian, H., Bahrami, G., Pourmanouchehri, Z., Hosseinzadeh, L., Mohammadi, B., Vosoughi, A., Forouhar, K., Behbood, L., 2022. Preparation and evaluation of extended-release nanofibers loaded with pramipexole as a novel oral drug delivery system: hybridization of hydrophilic and hydrophobic polymers. J. Pharm. Innov. https://doi.org/10.1007/s12247-022-09625-1.

Mercuri, N., Bernardi, G., 2005. The 'magic' of -dopa: why is it the gold standard Parkinson's disease therapy? Trends Pharmacol. Sci. 26, 341–344. https://doi.org/10.1016/j.tips.2005.05.002.

Montero-Padilla, S., Velaga, S., Morales, J.O., 2017. Buccal dosage forms: general considerations for pediatric patients. AAPS PharmSciTech 18, 273–282. https://doi.org/10.1208/s12249-016-0567-2.

Muthu, S., Uma Maheswari, J., Srinivasan, S., Isac paulraj, E., 2013. Spectroscopic studies, potential energy surface and molecular orbital calculations of pramipexole. Spectrochim. Acta Part A 115, 64–73. https://doi.org/10.1016/j.saa.2013.06.004.

Nair, A.B., Al-Dhubiab, B.E., Shah, J., Vimal, P., Attimarad, M., Harsha, S., 2018. Development and evaluation of palonosetron loaded mucoadhesive buccal films. J. Drug. Deliv. Sci. Technol. 47, 351–358. https://doi.org/10.1016/j.jddst.2018.08.014.

Pamlényi, K., Kristó, K., Jójárt-Laczkovich, O., Regdon, G., 2021. Formulation and optimization of sodium alginate polymer film as a buccal mucoadhesive drug delivery system containing cetirizine dihydrochloride. Pharmaceutics 13, 619. https://doi.org/10.3390/pharmaceutics13050619.

Pamlényi, K., Kristó, K., Sovány, T., Regdon jr., G., 2022. Development and evaluation of bioadhesive buccal films based on sodium alginate for allergy therapy. Heliyon 8, e10364. https://doi.org/10.1016/j.heliyon.2022.e10364.

Park, A., Stacy, M., 2009. Non-motor symptoms in Parkinson's disease. J. Neurol. 256, 293–298. https://doi.org/10.1007/s00415-009-5240-1.

Pfeiffer, R.F., 2016. Non-motor symptoms in Parkinson's disease. Parkinsonism Relat. Disord. 22, S119–S122. https://doi.org/10.1016/j.parkreldis.2015.09.004.

Poewe, W., Seppi, K., Tanner, C.M., Halliday, G.M., Brundin, P., Volkmann, J., Schrag, A.-E., Lang, A.E., 2017. Parkinson disease. Nat. Rev. Dis. Primers 3, 17013. https://doi.org/10.1038/nrdp.2017.13.

Shin, J.Y., Park, H.-J., Ahn, Y.H., Lee, P.H., 2009. Neuroprotective effect of l-dopa on dopaminergic neurons is comparable to pramipexol in MPTP-treated animal model of Parkinson's disease: a direct comparison study. J. Neurochem. 111, 1042–1050. https://doi.org/10.1111/j.1471-4159.2009.06381.x.

Sprenger, F., Poewe, W., 2013. Management of motor and non-motor symptoms in Parkinson's disease. CNS Drugs 27, 259–272. https://doi.org/10.1007/s40263-013-0053-2.

Sterzenbach, T., Helbig, R., Hannig, C., Hannig, M., 2020. Bioadhesion in the oral cavity and approaches for biofilm management by surface modifications. Clin. Oral. Invest 24, 4237–4260. https://doi.org/10.1007/s00784-020-03646-1.

Stowe, R., Ives, N., Clarke, C.E., van Hilten, Ferreira, J., Hawker, R.J., Shah, L., Wheatley, K., Gray, R., 2008. Dopamine agonist therapy in early Parkinson's disease. Cochrane Database Syst. Rev. https://doi.org/10.1002/14651858.CD006564.pub2.

Tzankov, B., Tzankova, V., Aluani, D., Yordanov, Y., Spassova, I., Kovacheva, D., Avramova, K., Valoti, M., Yoncheva, K., 2019. Development of MCM-41 mesoporous silica nanoparticles as a platform for pramipexole delivery. J. Drug Deliv. Sci. Technol. 51, 26–35. https://doi.org/10.1016/j.jddst.2019.02.008.

Whitton, A.E., Reinen, J.M., Slifstein, M., Ang, Y.-S., McGrath, P.J., Iosifescu, D.V., Abi-Dargham, A., Pizzagalli, D.A., Schneier, F.R., 2020. Baseline reward processing and ventrostriatal dopamine function are associated with pramipexole response in depression. Brain 143, 701–710. https://doi.org/10.1093/brain/awaa002.

Zanettini, R., Antonini, A., Gatto, G., Gentile, R., Tesei, S., Pezzoli, G., 2007. Valvular heart disease and the use of dopamine agonists for Parkinson's disease. N. Engl. J. Med. 356, 39–46. https://doi.org/10.1056/NEJMoa054830.